

Comparison of the thermal stabilities of NiSi films in Ni/Si, Ni/Pd/Si and Ni/Pt/Si systems

This article has been downloaded from IOPscience. Please scroll down to see the full text article.

2003 J. Phys.: Condens. Matter 15 1935

(<http://iopscience.iop.org/0953-8984/15/12/310>)

View [the table of contents for this issue](#), or go to the [journal homepage](#) for more

Download details:

IP Address: 171.66.16.119

The article was downloaded on 19/05/2010 at 08:29

Please note that [terms and conditions apply](#).

Comparison of the thermal stabilities of NiSi films in Ni/Si, Ni/Pd/Si and Ni/Pt/Si systems

R N Wang and J Y Feng¹

Key Laboratory of Advanced Materials, Department of Materials Science and Engineering, Tsinghua University, Beijing 100084, People's Republic of China

E-mail: fengjy@mail.tsinghua.edu.cn

Received 20 November 2002

Published 17 March 2003

Online at stacks.iop.org/JPhysCM/15/1935

Abstract

The effects of different interlayer materials (Pd and Pt) deposited between Ni films and Si substrates on the NiSi thermal stability are discussed. Ni_{0.943}Pd_{0.057}Si and Ni_{0.945}Pt_{0.055}Si solid solutions were formed when the samples were annealed at high temperatures and the lattice parameters of Ni_{0.943}Pd_{0.057}Si were calculated according to Vegard's law. The NiSi thermal stability was enhanced by interposing a Pd or Pt interlayer, and the sample with the Pt interlayer had the highest NiSi thermal stability among all the samples studied. This is attributed to the reduction of the interface energy between NiSi and Si substrates and the decrease of the driving force for the nucleation of NiSi₂, induced by formation of the NiSi(200) preferred orientation and the solid solution respectively.

1. Introduction

Silicides are essential in complementary metal oxide–semiconductor (CMOS) technology as local interconnect and contact materials. Currently, TiSi₂ is the material most widely used in such applications. However, the transformation from a high-resistivity C49-TiSi₂ phase to a low-resistivity C54-TiSi₂ phase becomes increasingly difficult as the linewidth decreases, leading to undesirable high sheet resistance for gate lines narrower than 0.35 μm [1–3]. Nickel mono-silicide (NiSi) has the potential for replacing C54-TiSi₂ and is becoming one of the basic materials in fabrication of ultralarge-scale integrated circuits [4, 5]. NiSi does not present the nucleation problem of C54-TiSi₂ [6, 7], nor does it show the Si consumption issue occurring in CoSi₂ fabrication. In addition, a one-step anneal can be used for the self-aligned silicide process [8]. However, the phase transition from NiSi to high-resistivity NiSi₂ at temperatures greater than 750 °C poses a serious problem [9]. In the past few years, much work has been done to improve the stability of NiSi films [10–15]. Recently, it has been demonstrated that

¹ Author to whom any correspondence should be addressed.

the addition of 5 at.% Pt into Ni films by using a $\text{Ni}_{0.95}\text{Pt}_{0.05}$ alloy target for film deposition can significantly improve the thermal stability of NiSi [10]. In our recent work, a Ni/Pt/Si bi-layered film was used instead of the Ni(Pt) alloy film in order to incorporate Pt into NiSi films and improve the thermal stability of the NiSi on Si(111) substrates [16].

In the present paper, the thermal stability of NiSi was investigated in the presence of an interlayer of Pd intercalated between Ni films and Si substrates. The effects of different interlayer materials (Pt and Pd) on the thermal stability of the system were also compared. The mechanism of the enhanced thermal stability was investigated by analysing the change in the interface energy between NiSi and Si substrates and the Gibbs free energy for NiSi_2 nucleation.

2. Experimental details

An 8 nm thin layer of Pd and a 100 nm thick layer of Ni were sequentially electron-gun evaporated on Si(111) substrates, forming a Ni/Pd/Si bi-layered film. The base pressure of the vacuum chamber was 1×10^{-8} Torr and, during the deposition, the vacuum was better than 3×10^{-8} Torr. Similarly, a Ni/Pt/Si bi-layered film was formed with the same experimental parameters, which were also adopted in [16]. For comparison, a 100 nm thick Ni film without the Pd or Pt interlayer was deposited under similar experimental conditions, forming a Ni/Si film. Henceforth the Ni/Si, Ni/Pd/Si and Ni/Pt/Si films will be called samples (a), (b) and (c), respectively. Rapid thermal annealing (RTA) of all the samples was carried out in a 3×10^{-6} Torr high vacuum at temperatures ranging from 700 to 900 °C for 2 min.

X-ray diffraction (XRD) and micro-Raman measurements were employed for identifying the phases and their orientation in relation to the Si substrates, during the silicidation reaction. Auger electron spectra (AES) were used to investigate the distribution profile of the elements in the films. The XRD observations were carried out with a D/max-RB instrument using the $\text{Cu K}\alpha$ line. The AES was recorded with a PHI-610 scanning Auger microprobe. The micro-Raman measurements were done on the annealed sample (c) with a 514 nm argon laser beam focused to a diameter of about 1 μm .

3. Results and discussion

All the samples were annealed at the same temperature and XRD analysis was carried out for each sample, as shown in figures 1 and 2. In the RTA-treated (a), (b) and (c) samples at 750 °C, pure polycrystalline NiSi films were formed (not shown in this paper), in agreement with the previous work [16]. When the annealing temperature was increased to 800 °C (figure 1(a)), the peaks corresponding to $\text{NiSi}_2(111)$ and (222) planes alone were present in sample (a), indicating that epitaxial NiSi_2 films were formed and the transition from NiSi to NiSi_2 had been completed. The samples (b) and (c) (figures 1(b) and (c)) showed no evidence of the phase transition at this temperature as the NiSi_2 diffraction peak was absent in the spectra. When samples (b) and (c) were annealed further at 900 °C, high-quality epitaxial NiSi_2 was obtained in sample (b) as indicated by the presence of a unique diffraction peak of $\text{NiSi}_2(111)$ (figure 2(a)). At this temperature, the $\text{NiSi}_2(111)$ peak also appeared in the XRD patterns of sample (c), but the strong diffraction peaks corresponding to NiSi were still present (figure 2(b)), indicating that the transition from NiSi to NiSi_2 was not yet completed. One can conclude from the experimental data that the thermal stability of NiSi was better in sample (b) than sample (a) (without the interlayer). Secondly, the Pd interlayer enhanced the thermal stability temperature of NiSi by 50 °C. Sample (c), with the Pt interlayer, was the most stable of the three samples, because NiSi was not completely transformed to NiSi_2 even upon annealing at 900 °C. The thin Pt

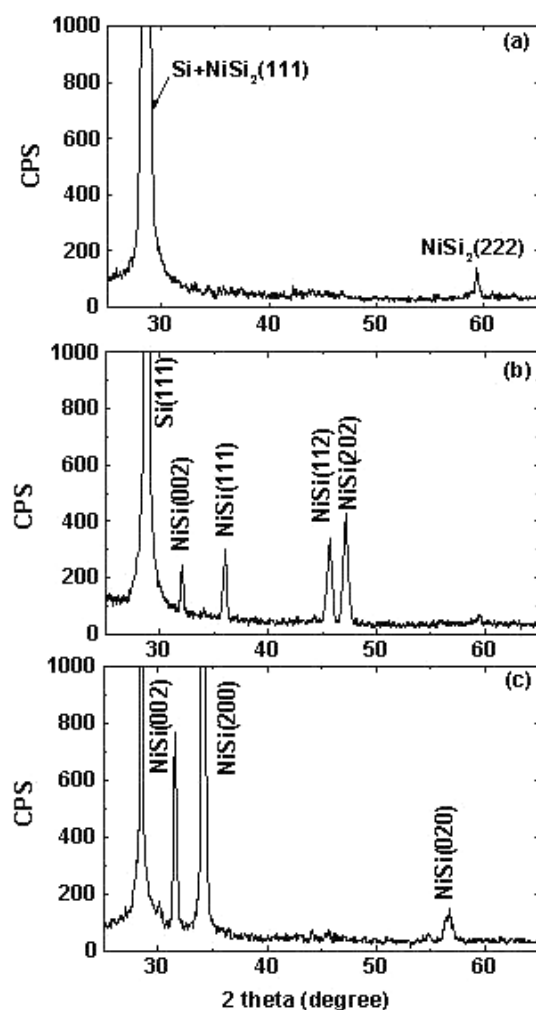


Figure 1. XRD patterns of the Ni/Si (a), Ni/Pd/Si (b) and Ni/Pt/Si (c) samples annealed at 800 °C for 2 min.

layer can improve the thermal stability temperature of NiSi as compared with sample (a) by at least 100 °C. This is also confirmed by micro-Raman measurements. The characteristic features of Raman spectra of various Ni silicide phases have been identified previously in a study of silicide formation on Si(100) substrates [17]. The dominant NiSi Raman peak at 212 cm^{-1} could be observed when sample (c) was annealed at 800 °C (figure 3(a)). The Raman peaks corresponding to NiSi₂ appeared beside the strong NiSi Raman peak when the annealing temperature rose to 900 °C (figure 3(b)), indicating that the transition from NiSi to NiSi₂ was not complete. All the micro-Raman measurements were consistent with the XRD results. One can therefore affirm that the presence of the Pt or Pd interlayer between Ni films and Si substrates improves the thermal stability of NiSi. The thermal stability of NiSi is best for the sample with the Pt interlayer (stable at about 900 °C).

The XRD patterns of sample (b) (figure 1(b)) show no peaks corresponding to PdSi. Comparing the positions of the NiSi diffraction peaks in figure 1(b) with those in [18], we found

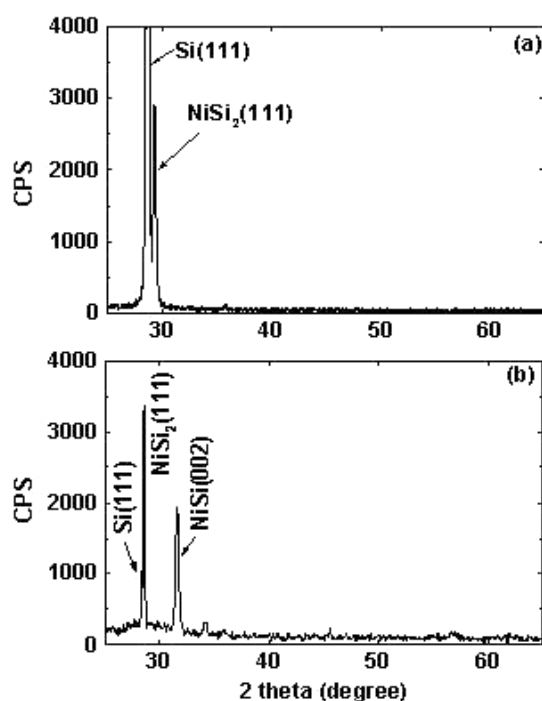


Figure 2. XRD patterns of the Ni/Pd/Si (a) and Ni/Pt/Si (b) samples annealed at 900 °C for 2 min.

Table 1. Comparison of the XRD peak positions of pure NiSi and Ni(Pd)Si solid solution (Cu K α irradiation).

	(111)		(112)		(202)	
	2θ (deg)	d (Å)	2θ (deg)	d (Å)	2θ (deg)	d (Å)
NiSi ^a	36.15	2.485	45.88	1.978	47.32	1.921
Ni(Pd)Si ^b	36.00	2.495	45.68	1.986	47.16	1.927
Ni(Pd)Si ^c	36.03	2.493	45.71	1.985	47.11	1.929

^a Data from [18].

^b Experimental data.

^c Calculated from the Vegard's law.

some subtle differences in peak positions which we list in table 1. These shifts are attributed to the formation of NiSi–PdSi solid solutions. Both NiSi and PdSi have an orthorhombic MnP structure, with the lattice constants $a = 5.233$ Å, $b = 3.258$ Å, $c = 5.659$ Å for NiSi [18] and $a = 5.599$ Å, $b = 3.381$ Å, $c = 6.133$ Å for PdSi [19]. Their lattice parameters differ, therefore, by no more than 15%. Thus NiSi–PdSi solid solutions can be formed for a wide range of concentrations. The original thicknesses of the Pd and Ni films were 8 and 100 nm respectively; it can be concluded that the atomic percentage of PdSi in the solid solution is 5.7 at.%. Applying Vegard's law indicates that the lattice parameters of the Ni_{0.943}Pd_{0.057}Si solid solution should be $a = 5.254$ Å, $b = 3.265$ Å and $c = 5.686$ Å. This result is in good agreement with the positions of the (111), (112) and (202) diffraction peaks of NiSi for the annealed sample (b) (figure 1(b)), as listed in table 1. Moreover, this conclusion was also

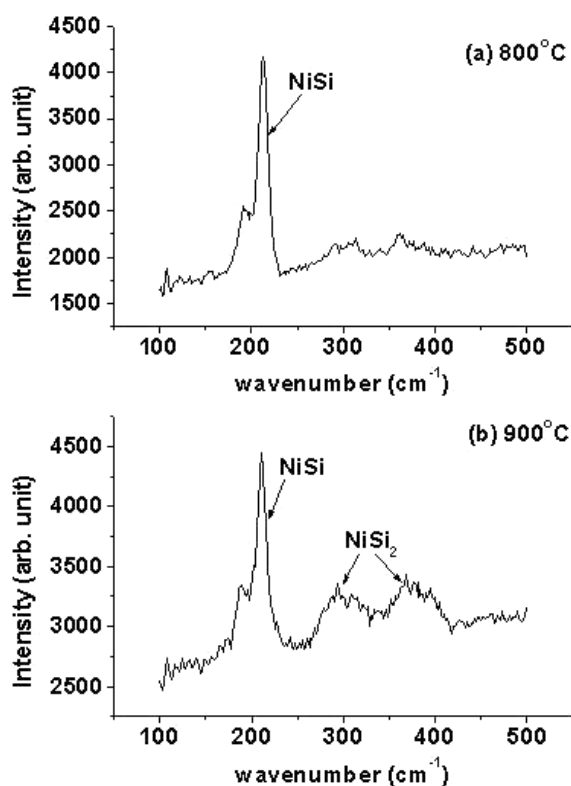


Figure 3. Micro-Raman analyses of the Ni/Pt/Si sample annealed at 800 °C (a) and 900 °C (b) for 2 min.

correlated with the AES depth profile (figure 4). As can be seen in figure 4(a), sample (b) (annealed at 800 °C) showed a uniform Pd distribution through the depth of the film although the Pd was deposited before the Ni. Concentration profiles of Ni and Si show that the ratio of Ni to Si is constant, which indicates the formation of stable Ni silicides. When the annealing temperature reached 900 °C, Ni atoms diffused further into the Si substrates and the ratio of Ni to Si was approximately equal to 1:2 (figure 4(b)), implying the formation of NiSi₂. These results were consistent with the XRD patterns in figures 1(b) and 2(a). In the case of sample (c), a NiSi–PtSi solid solution was formed when the sample was annealed at a high temperature [16]; consequently the atomic percentage of PtSi in the solid solution was 5.5 at.%. Therefore, the Pd or Pt interlayers seem to play a similar role in the transition from NiSi to NiSi₂. They form Ni_{1-x}M_xSi (M denotes Pd or Pt and *x* denotes the content of M) solid solutions, resulting in enhanced thermal stability of NiSi.

In a previous work [20], the effect of film thickness on the NiSi-to-NiSi₂ transition temperature in the Ni/Pt/Si(100) system was investigated and the nucleation of NiSi₂ in the presence of the solid solution was studied. As we know, the NiSi-to-NiSi₂ transition is a typical nucleation-controlled reaction:



The Gibbs free energy for this reaction is $\Delta G_0 = G_f(\text{NiSi}_2) - G_f(\text{NiSi}) - G_f(\text{Si})$. We believe the Ni_{1-x}Pd_xSi and Ni_{1-x}Pt_xSi solid solutions affect the NiSi₂ nucleation similarly.

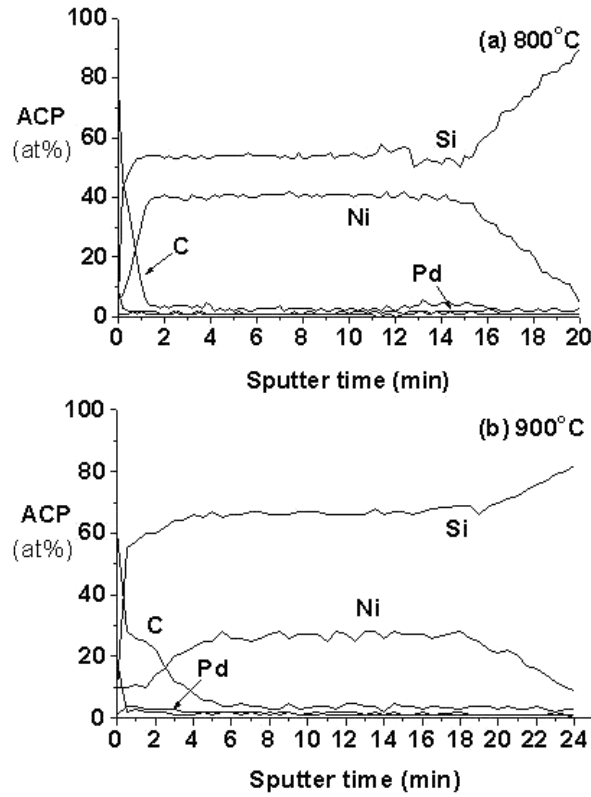


Figure 4. AES depth profiles of the Ni/Pd/Si sample annealed at 800 °C (a) and 900 °C (b) for 2 min.

According to [20], the formation of NiSi₂ in the presence of Ni_{1-x}M_xSi is modified as follows:



The Gibbs free energy for the reaction (2) is [20]

$$\Delta G_1 = (1-x)[G_f(\text{NiSi}_2) - G_f(\text{NiSi}) - G_f(\text{Si})] + T \Delta S_{mix} = (1-x) \Delta G_0 + T \Delta S_{mix} \quad (3)$$

where ΔS_{mix} denotes the mixing entropy for formation of the solid solution. Since the value of ΔG_0 is negative and the value of $T \Delta S_{mix}$ is positive [20], ΔG_0 is more negative than ΔG_1 , implying a larger driving force for reaction (1) than for reaction (2).

The activation energy for NiSi₂ nucleation is $\Delta G^* \cong \Delta \sigma^3 / \Delta G^2$, where $\Delta \sigma$ and ΔG stand for the change in the interface energy and the Gibbs free energy for the NiSi₂ nucleation reaction. Since $|\Delta G_1| < |\Delta G_0|$, we can reasonably expect a larger activation energy ΔG^* due to the presence of the Ni_{1-x}M_xSi solid solution. Therefore, NiSi₂ nucleation is harder to achieve in sample (b) or (c) with the metal interlayer than in sample (a) where the latter is absent. This indicates that a higher NiSi₂ formation temperature is needed for sample (b) or (c) and that NiSi has a higher thermal stability as compared with sample (a).

However, the NiSi in sample (b) was stable at 800 °C while the NiSi in sample (c) was stable at about 900 °C, at which temperature the transition from NiSi to NiSi₂ was completed in sample (b). The differences in NiSi thermal stability between samples (b) and (c) can be

Table 2. Comparison of the NiSi thermal stability in Ni/Pt/Si(111), Ni/Pd/Si(111) and Ni/Si(111) samples, considering the change in the energy σ of the interface between NiSi and Si substrates and the driving force $|\Delta G|$ for the NiSi₂ nucleation reaction.

	σ decrease?	$ \Delta G $ decrease?	Thermal stability sequence
Ni/Pt/Si(111)	Yes	Yes	1
Ni/Pd/Si(111)	No	Yes	2
Ni/Si(111)	No	No	3

attributed to the formation of a strong, preferred orientation NiSi(200) \parallel Si(111) in sample (c), as shown in figure 1(c). As was discussed in [16], the MnP-type structure can be expressed in terms of the NiAs structure (hexagonal, space group $P6_3/mmc$) if the ratio c/b equals $\sqrt{3}$ in the MnP structure. The addition of Pt decreases the c/b ratio from 1.7370 for pure NiSi to 1.7315 (close to $\sqrt{3}$) for Ni_{0.945}Pt_{0.055}Si, inducing the formation of the NiSi(200) texture [16]. The latter can reduce the energy σ of the interface between NiSi and the Si substrates and increase the change in the interface energy $\Delta\sigma$ for the NiSi₂ nucleation reaction. In the case of sample (b), an addition of Pd changes the ratio c/b in the MnP structure from 1.7370 for pure NiSi to 1.7415 (further from $\sqrt{3}$) for Ni_{0.943}Pd_{0.057}Si and no preferred orientations can be found in the XRD patterns of sample (b) (figure 1(b)), leaving the interface energy unchanged. Since the activation energy for the NiSi₂ nucleation $\Delta G^* \approx \Delta\sigma^3/\Delta G^2$, the texture induced by the addition of Pt leads to an increase in $\Delta\sigma$ and consequently in ΔG^* , making the NiSi films in sample (c) more stable than those in sample (b). The values of ΔG^* for different samples can be ordered as follows:

$$\Delta G^*(\text{Ni/Pt/Si}) > \Delta G^*(\text{Ni/Pd/Si}) > \Delta G^*(\text{Ni/Si}). \quad (4)$$

Therefore the NiSi in sample (c) is the most stable and samples (b) and (c) have higher NiSi thermal stability temperatures than sample (a). These results are consistent with our experiments.

From the above discussion, it follows that two important factors in the improvement of the NiSi thermal stability are the interface energy σ and the driving force $|\Delta G|$ for NiSi₂ nucleation. Both the reduction of σ between NiSi and the Si substrates and the decrease of $|\Delta G|$ are beneficial for blocking NiSi₂ formation because of the increase in the activation energy ΔG^* . The effects of these two factors on the improvement of the thermal stability of NiSi are listed in table 2.

4. Conclusions

In this paper, a comparison of the thermal stabilities of NiSi in Ni/Pt/Si, Ni/Pd/Si and Ni/Si samples is made. In the Ni/Pt/Si sample, both the Ni_{0.945}Pt_{0.055}Si solid solution and the preferred orientation NiSi(200) are observed, resulting in a decrease of the interface energy σ and a reduction of the driving force $|\Delta G|$ for the NiSi₂ nucleation reaction. In the Ni/Pd/Si sample, the NiPdSi solid solution is formed, leading to a decrease of $|\Delta G|$. According to the experimental data, the thermal stability of the textured NiSi films in the Ni/Pt/Si sample is higher than in its polycrystalline counterparts in the Ni/Pd/Si sample; also the sample with a Pt or Pd interlayer has more stable NiSi films than the sample without any interlayer. This shows that both reduction of the driving force $|\Delta G|$ and decrease of interface energy σ can improve the thermal stability of NiSi.

Acknowledgment

This work was supported by the National Natural Science Foundation of China.

References

- [1] Kittl J A, Prinslow D A, Apte P P and Pas M F 1995 *Appl. Phys. Lett.* **67** 2308
- [2] Zhang S L, Lavoie C, Cabral C, Harper J M, D'Heurle F M and Jordan-Sweet J 1999 *J. Appl. Phys.* **85** 2617
- [3] Saenger K L, Cabral J C, Clevenger L A, Roy R A and Wind S 1995 *J. Appl. Phys.* **78** 7040
- [4] Colgan E G, Gambino J P and Hong Q Z 1996 *Mater. Sci. Eng. R* **16** 43
- [5] Maex K 1993 *Mater. Sci. Eng. R* **11** 53
- [6] Beyers R and Sinclair R 1985 *J. Appl. Phys.* **57** 5240
- [7] Ma Z and Allen L H 1994 *Phys. Rev. B* **49** 13501
- [8] Morimoto T *et al* 1995 *IEEE Trans. Electron Devices* **42** 915
- [9] Julies B A, Knoesen D, Pretorius R and Adams D 1999 *Thin Solid Films* **347** 201
- [10] Mangelinck D, Dai J Y, Pan J S and Lahiri S K 1999 *Appl. Phys. Lett.* **75** 1736
- [11] Poon M C, Deng F, Chan M, Chan W Y and Lau S S 2000 *Appl. Surf. Sci.* **157** 29
- [12] Tsai C J, Chung P L and Yu K H 2000 *Thin Solid Films* **365** 72
- [13] Cheng L W, Chang S L, Chen J Y, Chen L J and Tsui B Y 1999 *Thin Solid Films* **356** 412
- [14] Poon M C, Chan M, Zhang W Q, Deng F and Lau S S 1998 *Microelectron. Reliab.* **38** 1499
- [15] Lee P S, Mangelinck D, Pey K L, Ding J, Chi D Z, Osipowicz T, Dai J Y and See A 2002 *Microelectron. Eng.* **60** 171
- [16] Liu J F, Chen H B, Feng J Y and Zhu J 2000 *Appl. Phys. Lett.* **77** 2177
- [17] Lee P S, Mangelinck D, Pey K L, Shen Z X, Ding J, Osipowicz T and See A 2000 *Electrochem. Solid State Lett.* **3** 153
- [18] D'Heurle F M, Peterson C S, Baglin J E E, La Placa S J and Wong C Y 1984 *J. Appl. Phys.* **55** 4208
- [19] Baxi H C and Massalski T B 1991 *J. Phase Equilib.* **12** 349
- [20] Liu J F, Feng J Y and Zhu J 2002 *Appl. Phys. Lett.* **80** 270